Polyhedron 50 (2013) 264–269

Contents lists available at SciVerse ScienceDirect

Polyhedron

journal homepage: www.elsevier.com/locate/poly

Nickel(II) complex of p-[*N*,*N*-bis(2-chloroethyl)amino]benzaldehyde-4-methyl thiosemicarbazone: Synthesis, structural characterization and biological application

Anitha Sankaraperumal [a], J. Karthikeyan [a,*], A. Nityananda Shetty [b], R. Lakshmisundaram [c]

[a] Department of Chemistry, Sathyabama University, Chennai 600 119, India
[b] Department of Chemistry, National Institute of Technology Karnataka, Mangalore 575 025, India
[c] Central Research Facility, Sri Ramachandra University, Chennai 600116, India

ARTICLE INFO

Article history:
Received 6 August 2012
Accepted 2 November 2012
Available online 28 November 2012

Keywords:
Ni(II) complex
Square planar complex
Thiosemicarbazone
SNNS donor type complex

ABSTRACT

New complex of Ni(II) with p-[*N*,*N*-bis(2-chloroethyl)amino]benzaldehyde-4-methyl thiosemicarbazone (CEAB-4-MTSC) have been synthesized and characterized by elemental analysis, IR, electronic, ^{1}H NMR spectroscopy. The crystal structure of the free ligand and complex has been determined by single crystal X-ray diffraction technique. In the complex, thiosemicarbazone ligand is coordinated to nickel through (1:2 complex) SNNS mode. The complex crystallizes in the triclinic with space group $P\bar{1}$. The complex has been tested for their antibacterial activity against various pathogenic bacteria. From this study, it was found out that the activity of complex reaches the effectiveness of the conventional bacteriocide Streptomycin compared to simple ligand.

1. Introduction

Thiosemicabazone {$R^1R^2C{=}N^3{-}N^2H{-}C(=S){-}NR^3R$} possess NNS donor atom and generally bind to metal via N^2, S or N^3, S donor atom forming four or five member ring, respectively. Thiosemicarbazones (TSC), as well as their metal complex, has been the subject of great interest of many researchers for a number of years. Apart from their diverse chemical and structural characteristics, the interest on these compounds also stems from their wide spectrum of biological activity. Their biological importance is evidenced by a wide range of antibacterial, antimalarial, antiviral, antineoplastic and antileprotic activities [1,2]. Such pharmacological activities are due to the strong chelating ability of this ligand with biologically important metal ions such as Fe, Cu, Ni and their reductive capacities [3–8]. Though the versatility of thiosemicarbazone ligand for binding to the metal ion has been well established elsewhere, there remains an ambiguity in predicting the actual coordination mode of thiosemicarbazone. As a part of continuing interest in this area of research, we have investigated coordination behaviour of square planar nickel(II) complex of thiosemicarbazone. The complex have been characterized by spectral and X-ray crystallography. With our keen interest in microbiological studies, based on the fact that metal complex are systematically more active to control pathogenic bacteria than the simple ligand by themselves, based on that new Ni(II) complex have been screened for their antibacterial activity against various pathogenic bacteria. The proposed metal complex contain aldehyde (nitrogen mustard–anticancer agent)–thiosemicarbazone (chemotherapeutic agent)–nickel (biologically important) metal link, so we are sure that the new synthetic compound will have a synergic effect to control pathogenic bacteria. These types of new therapeutic approach are rapidly emerging and further research may help in designing more specific chelates. Moreover, this complex is going to be a member of new larger family of complex with nickel(II) ion. This type of nickel(II)–thiosemicarbazone complex afford a wide variety of structure with associated conducting and magnetic properties and such complex has potential for use as building block in the preparation of novel molecular material with interesting conducting or magnetic properties [9,10]. The general reaction scheme (Scheme 1) for the preparation of the ligand in the present work is given below.

2. Experimental

2.1. Materials

All reagents and reactant were of analytical grade. The starting material p-[*N*,*N*-bis(2-chloroethyl)amino]benzaldehyde prepared by the reported procedure [11]. The purity of the compound checked by the elemental analysis and by melting point. 4-Methyl thiosemicarbazide, nickel salt was purchased from Aldrich and Merck respectively and were used as received.

* Corresponding author. Tel.: +91 44 22422776.
E-mail addresses: dr.j.karthikeyan@gmail.com, jkarthik_chem@rediffmail.com (J. Karthikeyan).

0277-5387/$ - see front matter © 2012 Elsevier Ltd. All rights reserved.
http://dx.doi.org/10.1016/j.poly.2012.11.006

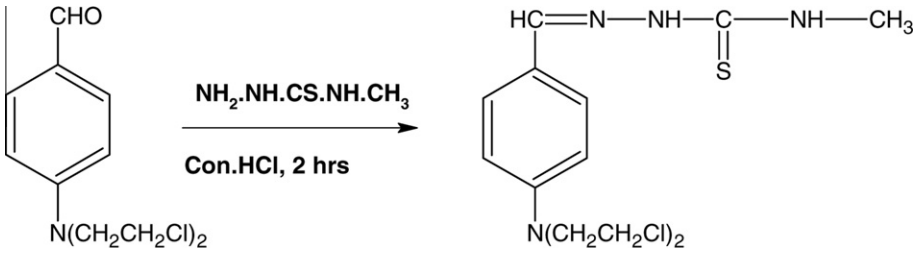

Scheme 1.

2.2. Measurements

Infrared spectral measurement were done on a Shimadzu DR 8001 series FTIR instrument using KBr pellets for spectra in the region 4000–400 cm^{-1}, and far IR spectra were recorded using polyethylene pellets in the 500–100 cm^{-1} region on a Nicolet magna 550 FTIR instrument. An ocean optics SD 2000 fiber optic spectrometer was used to measure solid-state reflectance spectra in the range 200–900 nm. ^1H NMR spectra were recorded using AMX 400 MHz FT-NMR Spectrometer with DMSO as solvent. EPR spectral measurements were carried out on a Varian E-112 X-band spectrometer using TCNE as standard. The magnetic susceptibility measurement were made using a simple Gouy balance at room temperature using mercury tetrathiocyanatocobaltate(II), $Hg[Co(NCS)_4]$ as calibrant.

2.3. Unit cell determination of the complex

X ray diffraction study was carried out using a Brukeraxs kappa Apx II single crystal CCD diffractometer equipped with Mo Kα (λ = 0.7107 Å) radiation. The goniometer equipped with the diffractometer is four circle goniometer with φ, χ, ω and 2θ axes by which the crystal is rotated. A crystal specimen of size 0.30 × 0.25 × 0.20 mm was cut and mounted on a glass fiber using cyano acrylate. The unit cell parameters were determined by collecting the diffracted intensities from 36 frames measured in three different crystallographic zones and using the method of difference vectors followed by data collection at 293 K using ω–φ scan modes.

2.4. Structure solution and refinement of the complex

The structure was solved by direct method using the program SHELXS 97[12], which revealed the position of all non-hydrogen atoms, and refined on F^2 by a full matrix least squares procedure using SHELXL 97. The non hydrogen atoms were refined anisotropically and the hydrogen atoms were allowed to ride over their parent atoms. The final cycle of refinement converged to R_1 = 0.0392 and wR_2 = 0.1056 for the observed reflections. The maximum and minimum heights in the final difference Fourier map were found to be 0.388 and −0.441 e $Å^{-3}$, respectively. Least squares planes and asymmetry calculations were done using the program PARST 97. The thermal ellipsoid plot and packing were done using ORTEP and PLATON, respectively [13,14]. Non bonded interaction graphics were created using the program PLATON. The crystallographic data and methods of data collection, solution and refinement are shown in Table 1 and selected bond distances and angles in Table 2. The atomic coordinates and equivalent isotropic displacement coefficients are included in the deposited material (CCDC – 817418 for ligand and 840170 for complex) as a complete list of bond distance and angle. In both the crystal structure of CEAB-4-MTSC and $[Ni(CEAB\text{-}4\text{-}MTSC)_2]$, all the 2-chloroethylamino group is disordered and is treated well during refinement. In CEAB-4-MTSC the 2-chloroethylamino group is positional disordered over two position with refined site occupancies of 0.696(5) and 0.304(5), respectively. Similarly for $[Ni(CEAB\text{-}4\text{-}MTSC)_2]$, the positional disordered 2-chloroethylamino group were refined to a site occupancies of 0.711(6) and 0.289(6) for $C_{10}C_{11}Cl_1$ and 0.721(2) and 0.283(2) for $C_{12}C_{13}Cl_2$, respectively. In both structure, bond distance of the minor component were made similar to the major components using certain similarity restraints with a standard of uncertainty of 0.01 and 0.02 Å, respectively. The positions of the entire hydrogen atom were identified from the differential electron density map and were allowed to ride on the parent atom.

2.5. Preparation of CEAB-4-MTSC ligand

The p-[*N*,*N*-bis(2-chloroethyl)amino]benzaldehyde-4-methyl thiosemicarbazone (CEAB-4-MTSC) was prepared by refluxing ethanol solution of p-[*N*,*N*-bis(2-chloroethyl)amino]benzaldehyde (20 mL) with 4-methylthiosemicarbazide (20 mL) in presence of hydrochloric acid (35%, 0.5 mL) taken into a 250 mL round bottom

Table 1
Crystal data and structure refinement of CEAB-4-MTSC and Ni (CEAB-4-MTSC)$_2$.

Parameters	CEAB-4-MTSC	Ni (CEAB-4-MTSC)$_2$
CCDC	CCDC 817418	CCDC 840170
Empirical formula	$C_{13}H_{18}Cl_2N_4S$	$C_{26}H_{34}Cl_4N_8NiS_2$
Formula weight	333.27	723.24
T (K)	293(2)	293(2)
λ (Å)	0.71073	0.71073
Crystal system, space group	triclinic, $P\bar{1}$	triclinic, $P\bar{1}$
Unit cell dimensions		
a (Å)	9.6538(4)	7.5947(5)
b (Å)	9.8404(4)	8.8875(8)
c (Å)	10.3659(4)	12.9688(8)
α (°)	94.306(2)	80.987(4)
β (°)	107.195(2)	80.934(4)
γ (°)	115.192(2)	65.842(4)
Z	2	2
D_{calc} (Mg/m^3)	1.337	1.531
Crystal size (mm)	0.30 × 0.25 × 0.20	0.30 × 0.25 × 0.20
$F(000)$	348	374
θ (°)	2.11–24.99	2.52–29.38
Limiting indices	$-11 \leqslant h \leqslant 11$, $-11 \leqslant k \leqslant 11$, $-12 \leqslant l \leqslant 12$	$-10 \leqslant h \leqslant 10$, $-11 \leqslant k \leqslant 12$, $-17 \leqslant l \leqslant 17$
Reflections collected/ unique (R_{int})	15128/2911 (0.0295)	18489/4293 (0.0287)
Refinement method	full-matrix least-squares on F^2	full-matrix least-squares on F^2
Data/restraints/ parameters	2911/7/211	4293/9/250
Goodness-of-fit (GOF) on F^2	1.045	1.006
Final R-indices [$I > 2\sigma(I)$]	R_1 = 0.0539, wR_2 = 0.1442	R_1 = 0.0392, wR_2 = 0.1056
R-indices (all data)	R_1 = 0.0766, wR_2 = 0.1642	R_1 = 0.0611, wR_2 = 0.1210
Largest diff. peak and hole (e $Å^{-3}$)	0.388 and −0.441	0.537 and −0.260

Table 2
Selected bond lengths (Å) and angles (°) of CEAB-4-MTSC and Ni (CEAB-4-MTSC)$_2$.

Bond length	CEAB-4-MTSC	Bond length	Ni (CEAB-4-MTSC)$_2$
C(1)–C(2)	1.498(6)	C(1)–N(2)	1.297(3)
C(2)–N(4)	1.439(6)	C(1)–N(3)	1.350(3)
N(4)–C(5)	1.391(5)	C(1)–S(1)	1.732(2)
N(4)–C(3)	1.464(5)	C(2)–N(3)	1.436(3)
C(3)–C(4)	1.473(6)	C(3)–N(1)	1.298(3)
C(5)–C(10)	1.392(4)	C(3)–C(4)	1.448(3)
C(5)–C(6)	1.400(4)	C(4)–C(5)	1.387(3)
C(6)–C(7)	1.362(4)	C(4)–C(9)	1.399(3)
C(7)–C(8)	1.388(4)	C(5)–C(6)	1.373(3)
C(8)–C(9)	1.386(4)	C(6)–C(7)	1.393(3)
C(9)–C(10)	1.370(4)	C(7)–N(4)	1.379(3)
C(8)–C(11)	1.450(4)	C(7)–C(8)	1.401(3)
C(11)–N(1)	1.271(4)	C(8)–C(9)	1.369(3)
C(12)–N(3)	1.320(4)	N(1)–N(2)	1.401(2)
C(12)–N(2)	1.344(4)	N(1)–Ni(1)	1.9195(16)
C(12)–S(1)	1.683(3)	N(4)–C(10)	1.440(9)
C(13)–N(3)	1.452(4)	N(4)–C(12)	1.487(4)
N(1)–N(2)	1.380(3)	S(1)–Ni(1)	2.1771(6)
		Ni(1)–N(1)$^{\#}$	1.9195(16)
		Ni(1)–S(1)$^{\#}$	2.1771(6)
		C(12)–C(13)	1.499(5)
		C(10)–C(11)	1.493(10)
Bond angles		Bond angles	
C(2)–C(1)–Cl(1)	105.2(4)	N(2)–C(1)–N(3)	119.10(19)
N(4)–C(2)–C(1)	112.4(4)	N(2)–C(1)–S(1)	123.65(16)
C(5)–N(4)–C(2)	122.4(4)	N(3)–C(1)–S(1)	117.25(16)
C(5)–N(4)–C(3)	120.6(3)	N(1)–C(3)–C(4)	132.6(2)
C(2)–N(4)–C(3)	116.7(4)	C(5)–C(4)–C(9)	116.36(19)
N(4)–C(3)–N(4')	23.6(4)	C(5)–C(4)–C(3)	117.33(19)
N(3)–C(12)–N(2)	116.3(3)	C(1)–S(1)–Ni(1)	95.46(7)
N(3)–C(12)–S(1)	124.1(2)	N(1)$^{\#}$–Ni(1)–N(1)	179.999(2)
N(2)–C(12)–S(1)	119.6(2)	N(1)$^{\#}$–Ni(1)–S(1)	94.40(5)
C(12)–N(2)–N(1)	120.0(3)	N(1)–Ni(1)–S(1)	85.60(5)
C(11)–N(1)–N(2)	116.0(3)	N(1)–Ni(1)–S(1)$^{\#}$	94.40(5)

flask. The mixture was refluxed for around 2 h and cooled, after cooling, a yellow precipitate appeared, filtered, washed with ethanol followed by ether. The compound is recrystallized using small amount of ethanol to get pure shiny yellow crystals suitable for X-ray crystallography. [Analysis results for $C_{13}H_{18}Cl_2N_4S$. Found, FT-IR (KBr): 3375 cm^{-1}(ν_{N-H}), 1604 cm^{-1} ($\nu_{C=N}$), 813 cm^{-1} ($\nu_{C=S}$). The ^{1}H NMR data for compound show that the N–H and azomethine (–CH=N–) protons are observed as singlet 11.26 and 7.92 ppm, respectively. While the phenyl protons of the compound gave a multiplet at δ = 6.76–7.62 ppm. The signals due to the –CH_2–CH_2– protons are gave a multiplet at δ = 3.00–3.80 ppm].

2.6. Preparation of new [Ni(CEAB-4-MTSC)$_2$] complex

A mixture of $NiCl_2{\cdot}6H_2O$ (1 mmol) and CEAB-4-MTSC (2 mmol) in ethanol was stirred for around 4 h using magnetic stirrer at room temperature, after which it was set aside, overnight when an dark brown crystalline product separated out, which was filtered, washed with cold ethanol and dried in vacuo. Dark brown crystals suitable for X-ray diffraction study were obtained for the nickel complex by slow evaporation of its DMSO solution.

2.7. Bacterial strains

The following bacteria and fungi were used for the experiment. *Staphylococcus aureus* MTCC 96, *Micrococcus*, *Shigella flexneri* MTCC 1457, *Staphylococcus epidermidis* MTCC 3615, *Proteus vulgaris* MTCC 1771, *Pseudomonas aeruginosa* MTCC 741, *Klebsiellap neumonia* MTCC 109, *Salmonella typhimurium* MTCC 1251, *Bacillus subtilis* MTCC 441, *Salmonella paratyphi-B* and *Staphylococcus aureus* (MRSA-methicillin resistant, clinical pathogen) were used. *Candida albicans* MTCC 227, *Malassesia pachydermatis* and *Trichophyton mentagrophytes* 66/01 were used for antifungal activities. The reference cultures were obtained from Institute of Microbial Technology (IMTECH – CSIR), Chandigarh, India 160 036. All the cultures were obtained from the Department of Microbiology, Christian Medical College, Vellore, Tamil Nadu, India. Bacterial inoculums were prepared by growing cells in Mueller Hinton broth (MHB) (Himedia) for 24 h at 37 °C. The filamentous fungi were grown on sabouraud dextrose agar (SDA) slants at 28 °C for 10 days and the spores were collected using sterile doubled distilled water and homogenized. Yeast was grown on sabouraud dextrose broth (SDB) at 28 °C for 48 h.

2.8. Antimicrobial assay

Antibacterial and antifungal activity was carried out using disc-diffusion method [15]. Petri plates were prepared with 20 mL of sterile Mueller Hinton Agar (MHA) (Hi-media, Mumbai). The test cultures were swabbed on the top of the solidified media and allowed to dry for 10 min and a specific amount (25 μL from the 40 mg/mL) of compound was added to each disc. The loaded discs were placed on the surface of the medium and left for 30 min at room temperature for compound diffusion. Negative control was prepared using respective solvents. Streptomycin (10 μg/disc) was used as positive control. The plates were incubated for 24 h at 37 °C for bacteria and for 48 h at 28 °C for fungi. Zones of inhibition were recorded in milli meters and the experiment was repeated twice.

2.9. Minimum inhibitory concentration (MIC)

Minimum inhibitory concentration studies of synthesis compound were performed according to the standard reference method for bacteria [16], for filamentous fungi (CLSI, 2008) and yeasts (NCCLS/CLSI, 2002). The required concentrations (1000, 500, 250, 125, 62.5, 31.25 and 15.62 μg/mL) of the compound and fractions were dissolved in DMSO (2%), and diluted to give serial twofold dilutions that were added to each medium in 96 well plates. An inoculum of 100 from each well was inoculated. The antifungal agents Ketoconazole for fungi and Streptomycin for bacteria were included in the assays as positive controls. For fungi, the plates were incubated for 48–72 h at 28 °C and for bacteria the plates were incubated for 24 h at 37 °C. The MIC for fungi was defined as the lowest extract concentration, showing no visible fungal growth after incubation time. 5 μL of tested broth was placed on the sterile MHA plates for bacteria and incubated at respective temperature. The MIC for bacteria was determined as the lowest concentration of the compound inhibiting the visual growth of the test cultures on the agar plate.

3. Results and discussion

3.1. Spectral and magnetic measurements

IR spectrum of the complex was compared with those of the ligand in order to find out the point of attachment of the ligand to the metal ion in the complex. The IR spectrum of the free Schiff base ligand showed a strong absorption at around 1622–1595 cm^{-1} due to the azomethine ν(C=N) group. This absorption has been shifted to lower frequency in the complex indicating the coordination of the azomethine nitrogen to nickel ion [17,18]. The presence of a new band in the region 440–450 cm^{-1} due to ν(Ni–N) is another indication nitrogen of azomethine group in coordination. The ν(C–S) band that appeared at around 815 cm^{-1} in the free Schiff

Scheme 2.

bases disappeared completely and a new band appeared in the region 738–756 cm^{-1} attributed to the enolisation of NH–C═S group and subsequent coordination through the sulphur atom due to metal complex.

The ^1H NMR data for parent ligand shows singlet at 11.26 ppm due to the hydrazide N–H group. Absence of this signal in the spectra of the metal complexes confirms deprotonation of the thiosemicarbazone chain and subsequent coordination through the thiolato form. Azomethine (–CH═N–) proton are observed as doublet at 7.99 and 8.00 ppm, respectively. While the phenyl proton of the compound gave a multiplets at δ = 6.60–7.24 ppm. The signals due to the $-CH_2-CH_2-$ proton are gave a multiplets at δ = 3.00–3.80 ppm. There is no sign of a signal from thiol (–SH) group, which would be expected around 4 ppm [19] strongly confirm thione form.

The UV–Vis absorption spectrum of the brown colour Ni(II) complex in DMSO medium in the region around 200–900 nm displayed mainly three bands in the region 265 nm (37735 cm^{-1}), 375 nm (26666 cm^{-1}) and at 460 nm (21739 cm^{-1}). These bands may be assigned to three spin allowed transitions $^1A_{1g}\rightarrow{}^1Eg$, $^1A_{1g}\rightarrow{}^1A_{2g}$ and $^1A_{1g}\rightarrow{}^1B_{1g}$, respectively. The bands in the region around 26000 cm^{-1} are due to S→Ni(II) charge transfer transition (LMCT) and are primarily responsible for brown color of the Ni(II) complex. Absence of bands below 10000 cm^{-1} confirms square-planar nature of the complex, consistent with low spin and diamagnetic (μ_{eff} = 0.00 BM) nature [20–26].

3.2. X-ray crystallography

3.2.1. Crystal structure of the ligand CEAB-4-MTSC

Thiosemicarbazone exist in two tautomeric form, thione (A) and thiol (B) (Scheme 2). The thione function as bidentate neutral ligand and the thiol can deprotonate and act as an anionic ligand. Due to the presence of C═N, thiosemicarbazone exist as E and Z stereoisomer. Considering the thermodynamic stability, E isomer will predominate in the mixture [27]. The crystal structure reveal that the compound exist in the thione form and C11 and C12 are at E configuration to each other with respect to N1–N2 bond. The thione form in the solid state is strongly confirmed by the observed bond length C12–S1 [1.683(3) Å], C12–N2 [1.344(4) Å] and C12–N3 [1.320(4) Å]. The C12–S1 distance of 1.683(3) Å is closer to C═S bond length [1.62 Å] than to C–S bond length [1.81 Å], and C12–N2, C12–N3 distance of 1.344(4) and 1.325(6) Å respectively is in the range of 1.349(6)–1.386(4) Å for other thiosemicarbazone having C–N single bond reported earlier [28,29]. The shorter than usual length of C–N and longer than usual length of C═S point out the extended conjugation in the molecule, However, the N(1)–N(2) [1.380(3) Å], N(2)–C(12) [1.344(4) Å] and C12–N3 [1.325(6) Å] bond distance observed are intermediate between the ideal value of corresponding single [N–N, 1.45 Å; C–N, 1.47 Å] and double bond [N═N, 1.25 Å; C═N, 1.28 Å] which are in support of an extended 'π' delocalization along the thiosemicarbazone chain [30–32]. The angle around the atom of N1 is 359.7° and dihedral angle between the benzene ring to the thiourea and *N*,*N*-bis(2-chloroethyl)amino moiety is 13.12° and 6.90°, respectively, strongly confirming that the atom N(1) is in sp^2 hybridized state and the both group are lie in the same plane, due to the presence of hetero π–electron delocalization in the entire molecule [33]. The bond length of C5–C6, C5–C10, C7–C8, and C8–C9 in CEAB-4-MTSC molecule are 1.400(4), 1.392(4), 1.388(4) and 1.386(4) Å, respectively, these length are considerably higher than the normal value of 1.37 Å. These bond length variation are attributed to the resonance character of the methyl amine, phenyl ring and also that of imine nitrogen. In the title compound, bis(2-chloroethyl) amino moiety is disordered over two positions. The atoms $N_4–C_2–C_1–Cl_1$ and its disordered component $N'_4–C'_2–C'_1–Cl'_1$ exist in two position with percentage of occupancy 70% and 30%, respectively, whereas the position of the atom Cl_2 and its disordered component Cl_2' has the percentage of occupancy 67% and 33%, respectively. The Ortep diagram of the title compound with 40% ellipsoid probability showing the disordered component in Fig. 1.

3.2.2. Crystal structure of the complex [Ni(CEAB-4-MTSC)$_2$]

On the basis of the charge balance, bond distance and geometry of the ligand, the crystal structure of the complex indicate that the thiosemicarbazone ligand has lost a proton from its tautometric thiol form and act as a single negatively charged bidentate ligand coordinating to the nickel ion via the mercapto sulfur and β-nitrogen atom. The geometry around Ni(II) is almost square-planar with two equivalent Ni–N and two equivalent Ni–S bond, consists of neutral molecule [Ni(CEAB-4-MTSC)$_2$], with nickel at the centre of symmetry. Crystal structure of the complex is shown in Fig. 2. The Ni–S bond length is 217.71 pm, while the Ni–N bond length is 191.95 pm with the coordination sphere approaching a square planar configuration, which involves the thiolato sulfur atom and the imine nitrogen atom N1 of the two ligand in trans-configuration. In the free ligand, however, these centres are in trans configuration, indicating that the complexation occurs after a 180° rotation around the C1–N2 bond. As the ligand is deprotonated on N2 atom, a negative charge appears and is delocalized along the thiosemicarbazone moiety. This fact is confirmed by the difference between the bond distance in the deprotonated ligand of nickel complex

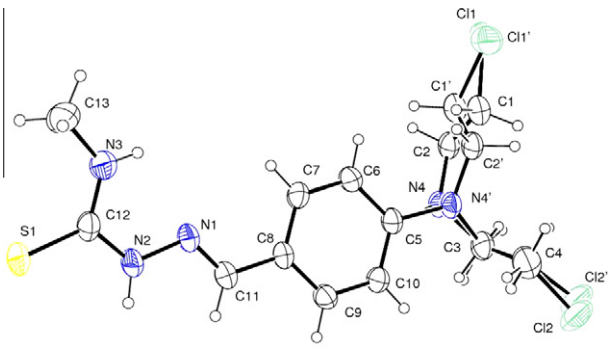

Fig. 1. Crystal structure of CEAB-4-MTSC.

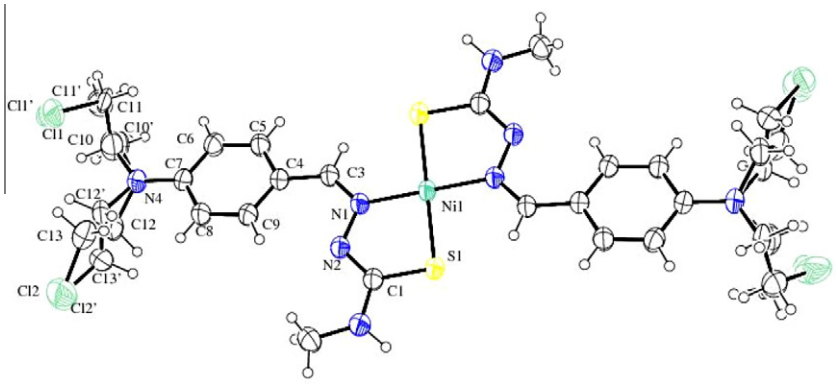

Fig. 2. Crystal structure of Ni(CEAB-4-MTSC)$_2$.

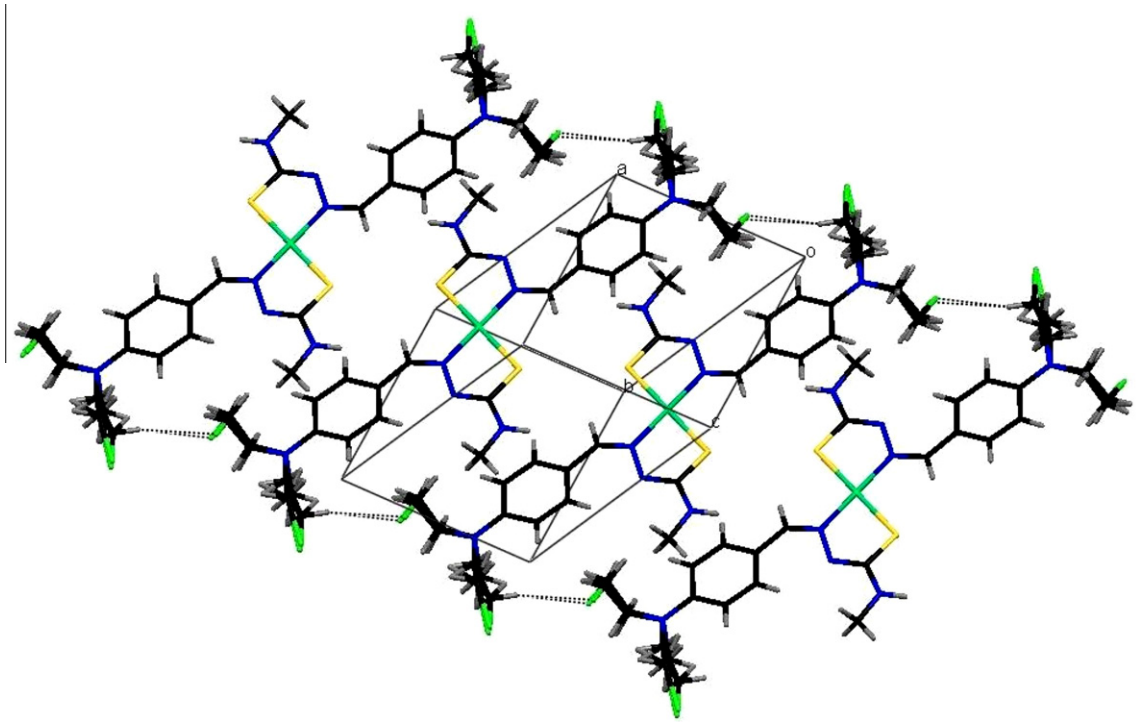

Fig. 3. Crystal packing of Ni(CEAB-4-MTSC)$_2$–H-bond contacts shown by dashed lines.

is C1–S1 = 1.732(2) Å (thiolato form); C1–N2 = 1.297(3) Å; C3–N1 = 1.298(3) Å and the same bond distance in the free ligand is C1–S1 = 1.683(3) Å (thione form); C1–N2 = 1.344(4) Å; C3–N1 = 1.271(4) Å. In the crystal, molecule are linked through intermolecular C–H···Cl hydrogen bond, generate edge fused ring motif. The hydrogen bonded motifs are linked to each other to form a three dimensional network, seems to be effective in the stabilization of the crystal structure to form chain [34]. Packing arrangement shown in Fig. 3. Polar hydrogen atom on the title thiosemicarbazone fragment, on C(13′)–H(13C) participating the hydrogen bond. Symmetry transformation used to generate dimensions of the hydrogen bond equivalent atom $x-1$, y, z, shows that d(D–H), d(H···A), d(D···A), <(DHA) are 0.97, 2.69, 3.603(9) Å and 156.4°, respectively. The conformation of thiosemicarbazone fragment is such that the imine N atom is oriented in a way to form an intermolecular hydrogen bond C(13′)–H(13C) ···Cl(1′) resulting in the formation of edge fused ring motif.

3.3. Biological activity

The antimicrobial screening data show that the compounds exhibit antimicrobial properties, and it is important to note that the nickel complex exhibit more inhibitory effect than the parent ligand. It is clear that the zone of inhibition is much larger for metal complex against the Gram-positive bacteria and Gram-negative bacteria (Table 3). The increased activity of the metal chelate can be explained on the basis of chelation theory. It is known that chelation tends to make the ligand act as more powerful and potent bactericidal agent, thus killing more of the bacteria than the ligand. It is observed that, π–electron delocalization over the whole complex increases the lipophilic character of the metal chelate and favours its permeation through the lipoid layer of the bacterial membrane [35–38]. There are other factors which also increase the activity, which are solubility, conductivity, and bond length between the metal and the ligand.

Table 3
Antimicrobial activity using the disc-diffusion method (zone of inhibition in mm).

Organism	CEAB-4-MTSC	Ni (CEAB-4-MTSC)$_2$	Streptomycin
Bacteria			
Staphylococcus aureus	9	12	14
Micrococcus	10	18	26
Shigella flexneri	9	18	30
Staphylococcus epidermidis	8	11	14
Proteus vulgaris	11	18	30
Salmonella typhimurium	8	18	24
Salmonella paratyphi-B	–	–	18
Pseudomonas aeruginosa	–	–	30
Bacillus subtilis	–	–	22
Klebsiella pneumonia	10	17	20
Staphylococcus aureus (MRSA)	8	14	–
Fungi			Ketoconazole
Candida albicans	8	20	28
Malassesia pachydermatis	10	19	29
Trichophyton mentagrophytes	–	–	30

(–) No activity; Streptomycin – standard antibacterial agent; Ketoconazole – standard antifungal agent.

Table 4
Minimum inhibitory concentration (μg/mL) against the tested bacteria and fungi.

Organism	CEAB-4-MTSC	Ni (CEAB-4-MTSC)$_2$	Streptomycin
Bacteria			
Staphylococcus aureus	125	100	6.25
Micrococcus	250	150	6.25
Shigella flexneri	250	150	6.25
Staphylococcus epidermidis	500	300	25
Proteus vulgaris	250	250	6.25
Salmonella paratyphi-B	500	200	–
Salmonella typhimurium	–	–	30
Pseudomonas aeruginosa	–	–	25
Bacillus subtilis	–	–	25
Klebsiella pneumonia	250	250	6.25
Staphylococcus aureus (MRSA)	500	250	–
Fungi			Fluconazole
Candida albicans	250	250	>100
Malassesia pachydermatis	250	250	12.5
Trichophyton mentagrophytes	–	–	25

(–) No activity; Streptomycin and Fluconazole (standard antimicrobial agent).

The results of fungicidal screening show that Ni(II) complex were highly active than the free ligand against phytopathogenic fungi, *C. albicans*, *M. pachydermatis*, and *T. mentagrophytes* (Table 4). The mode of action may involve the formation of a bond through the azomethane nitrogen atom with the active centres of the cell constituent, resulting in interference with the normal cell process. The variation in the effectiveness of different compound against different organism depends either on the impermeability of the cells of the microbes or the difference in ribosomes of microbial cells. It has also been proposed that concentration plays a vital role in increasing the degree of inhibition, as the concentration increases, the activity increases. It is noteworthy that the compound is effective against fungi and bacteria make it interesting for a practical use as antimicrobial agent.

4. Conclusion

New complex of Ni(II) with p-[*N*,*N*-bis(2-chloroethyl)amino] benzaldehyde-4-methyl hiosemicarbazone have been synthesized and characterized by elemental analysis, IR, electronic, ^{1}H NMR spectroscopy. The crystal structure of the free ligand and complex has been determined by single crystal X-ray diffraction technique. In the complex, thiosemicarbazone ligand is coordinated to nickel via (1:2 complex) SNNS mode. In the crystal, molecules are linked through intermolecular C–H···Cl hydrogen bond network, generate edge fused ring motif that stabilizes the crystal structure. The metal complex has shown enhanced synergic effect to control pathogenic bacteria comparable with standard Streptomycin.

Appendix A. Supplementary material

CCDC 817418 and 840170 contain the supplementary crystallographic data for ligand and complex, respectively. These data can be obtained free of charge via http://www.ccdc.cam.ac.uk/conts/retrieving.html, or from the Cambridge Crystallographic Data Centre, 12 Union Road, Cambridge CB2 1EZ, UK; fax: +44 1223 336 033; or e-mail: deposit@ccdc.cam.ac.uk.

Reference

[1] D.G. Bauer (Ed.), International Encyclopedia of Pharmacology, vol. 1, Pergamon Press, Oxford, 1972, p. 35.
[2] D.R. Williams, Chem. Rev. 72 (1972) 203.
[3] E. Sorkin, W. Roth, H. Erlenmeyer, Helv. Chim. Acta 35 (1952) 1736.
[4] J.C. Cymerman, D. Wills, S.D. Rubbo, J. Edgar, Nature 176 (1955) 34.
[5] S. Padhye, G.B. Kaufman, Coord. Chem. Rev. 63 (1985) 127.
[6] M.J.M. Cambell, Coord. Chem. Rev. 15 (1975) 279.
[7] S.K. Chattopadhyay, M. Hossain, A.K. Guha, S. Ghosh, Transition Met. Chem. 15 (1990) 473.
[8] G.J. Palenik, D.F. Rendle, W.S. Carter, Acta Crystallogr. Sect. B 30 (1974) 2390.
[9] R. Kato, Chem. Rev. 104 (2004) 5319.
[10] N. Robertson, L. Cronin, Coord. Chem. Rev. 227 (2002) 93.
[11] R.C. Elderfield, I.S. Covey, J.B. Geiduschek, W.L. Meyer, A.B. Ross, J.H. Ross, Potential Anticancer Agents 23 (1958) 1749.
[12] G.M. Sheldrick, Acta Crystallogr. Sect. A A64 (2008) 112.
[13] L.J. Farrugia, J. Appl. Crystallogr. 30 (1997) 565.
[14] A.L. Spek, J. Appl. Crystallogr. 36 (2003) 7.
[15] A.D. Weber, C.S. Sanders, Antimicrob. Agents Chemother. 34 (1990) 156.
[16] V. Duraipandiyan, P. Kanan, S. Ignacimuthu, Leaflets 13 (2009) 320.
[17] L.J. Baucher, J. Inorg. Nucl. Chem. 36 (1974) 531.
[18] J. Uttamachandani, R.N. Kapoor, Transition Met. Chem. 3 (1978) 79.
[19] D. Gattegno, A.M. Giuliani, Tetrahedron 30 (1974) 701.
[20] M.B. Ferrari, S. Capacchi, F. Bisceglie, G. Pelosi, P. Tarasconi, Inorg. Chim. Acta 312 (2001) 81.
[21] N.C. Kasuga, K. Sekino, C. Koumo, N. Shimala, M. Ishikawa, K. Nomiya, J. Inorg. Biochem. 84 (2001) 55.
[22] Alessia Famengo, Dalice Pinero, Olivier Jeannin, Thierry Guizouarn, Marc Fourmigue, Dalton Trans. 41 (2012) 1441.
[23] Xing Chen, Wei Qiang Chen, Lin Liang Yu, Jing Hua Lin, Dong Dong Zhou, Wen Tao Yin, Hong Rong Zuo, Jia Rong Zhou, Le Min Yang, Chun Lin Ni, J. Mol. Struct. 1006 (2011) 419.
[24] Anant Prakash, P.K. Mukesh, K.K. Singh, J. Dev. Biol. Tissue Eng. 3 (2) (2011) 13.
[25] V.M. Leovac, L.S. Jovanovic, V. Divijakovic, A. Pevec, I. Leban, T. Armbruster, Polyhedron 26 (2007) 49.
[26] K.R. Krishnapriya, M. Kandasamy, Polyhedron 24 (2005) 113.
[27] D.X. West, A.E. Liberta, S.B. Pandhye, R.C. Chikate, P.B. Sonawane, A.S. Kumbhar, R.G. Yerande, Coord. Chem. Rev. 123 (1993) 49.
[28] E. Huheey, E.A. Keiter, R.L. Keiter, Inorganic Chemistry Principles of Structure and Reactivity, fourth ed., Harper Collins College Publishers, New York, 1993.
[29] M. Joseph, V. Suni, M.R.P. Kurup, M. Nethaji, A. Kishore, S.G. Bhat, Polyhedron 23 (2004) 3069.
[30] A. Sreekanth, S. Sivakumar, M.R.P. Kurup, J. Mol. Struct. 655 (2003) 47.
[31] E.B. Seena, M.R.P. Kurup, Polyhedron 26 (2007) 829.
[32] A. Sreekanth, H.K. Fun, M.R.P. Kurup, J. Mol. Struct. 737 (2005) 61.
[33] V. Philip, V. Suni, M.R.P. Kurup, M. Nethaji, Polyhedron 23 (2004) 1225.
[34] N. Sampath, Rita Mathews, M.N. Ponnuswamy, Lin-Woo Kang, Mol. Cryst. Liq. Cryst. 518 (1) (2010) 151.
[35] Yu.-Mei. Hao, Acta Crystallogr. Sect. E 66 (2010) 2528.
[36] S.K. Sengupta, O.P. Pandey, B.K. Srivastava, V.K. Sharma, Transition Met. Chem. 23 (4) (1998) 349.
[37] S.O. Podunavac kuzmanovic, V.M. Leovac, N.U. Perisic janjic, J. Rogan, G. Balas, J. Serb. Chem. Soc. 64 (1999) 381.
[38] A. Wissner, D.M. Berger, D.H. Boschelli, J. Med. Chem. 43 (17) (2000) 3244.